Proc. Natl. Acad. Sci. USA
Vol. 93, pp. 7464–7469, July 1996
Biochemistry

In vitro activation of CPP32 and Mch3 by Mch4, a novel human apoptotic cysteine protease containing two FADD-like domains

(granzyme B/Mch2/protease cascade/FAS/APO-1-receptor)

TERESA FERNANDES-ALNEMRI*, ROBERT C. ARMSTRONG†, JOSEPH KREBS†, SRINIVASA M. SRINIVASULA*, LIJUAN WANG*, FLORENCIA BULLRICH*, LAWRENCE C. FRITZ†, JOSEPH A. TRAPANI‡, KEVIN J. TOMASELLI†, GERALD LITWACK*, AND EMAD S. ALNEMRI*§

*Center for Apoptosis Research and the Kimmel Cancer Institute, Jefferson Medical College, Philadelphia, PA 19107; †IDUN Pharmaceuticals, San Diego, CA 92121; ‡Cellular Cytotoxicity Laboratory, The Austin Research Institute, Heidelberg, Australia

Communicated by Sidney Weinhouse, Thomas Jefferson University, Philadelphia, PA, April 23, 1996 (received for review March 4, 1996)

ABSTRACT **Emerging evidence suggests that an amplifiable protease cascade consisting of multiple aspartate-specific cysteine proteases (ASCPs) is responsible for the apoptotic changes observed in mammalian cells undergoing programmed cell death. Here we describe the cloning of two novel ASCPs from human Jurkat T-lymphocytes. Like other ASCPs, the new proteases, named Mch4 and Mch5, are derived from single chain proenzymes. However, their putative active sites contain a QACQG pentapeptide instead of the QACRG present in all known ASCPs. Also, their N termini contain FADD-like death effector domains, suggesting possible interaction with FADD. Expression of Mch4 in *Escherichia coli* produced an active protease that, like other ASCPs, was potently inhibited (K_i = 14 nM) by the tetrapeptide aldehyde DEVD-CHO. Interestingly, both Mch4 and the serine protease granzyme B cleave recombinant proCPP32 and proMch3 at a conserved IXXD-S sequence to produce the large and small subunits of the active proteases. Granzyme B also cleaves proMch4 at a homologous IXXD-A processing sequence to produce mature Mch4. These observations suggest that CPP32 and Mch3 are targets of mature Mch4 protease in apoptotic cells. The presence of the FADD-like domains in Mch4 and Mch5 suggests a role for these proteases in the Fas-apoptotic pathway. In addition, these proteases could participate in the granzyme B apoptotic pathway.**

Apoptosis is a fundamental biochemical cell-death pathway essential for normal tissue homeostasis, cellular differentiation, and development within a multicellular organism (for review, see refs. 1–3). Members of the growing family of aspartate-specific cysteine proteases (ASCPs) that include mammalian interleukin 1β converting enzyme (ICE) (4, 5), Nedd2 (ICH-1) (6, 7), CPP32 (8), Mch2 (9), Mch3 (10), TX (ICH-2, ICErel-II) (11–13), and ICErel-III (13) have been implicated as mediators of all apoptotic cell death (for review, see ref. 14).

Cytotoxic T lymphocytes (CTL) induce apoptosis in their target cells possibly by activating members of the ASCP family (15). This hypothesis was supported by the observation that granzyme B, the CTL granule aspartate-specific serine protease, can cleave CPP32 (16). Recent observations suggested that the Fas-interacting protein FADD/MORT1 (17, 18) might also be connected to ASCP activation (19). Here we report the identification and cloning of two novel ASCP family members, which are named Mch4 and Mch5. Mch4 and Mch5 are unique in having an R to Q substitution in the QACRG pentapeptide active site motif conserved in all members of the ASCP family. We show that recombinant Mch4 is capable of processing the CPP32 and Mch3 proenzymes. We demonstrate that granzyme B cleaves CPP32, Mch3, and the newly identified Mch4 at an IXXD site conserved in all three proteins. Both Mch4 and Mch5 contain N-terminal FADD-like domains, suggesting that these ASCPs might be components of the Fas-apoptotic pathway.

The publication costs of this article were defrayed in part by page charge payment. This article must therefore be hereby marked "*advertisement*" in accordance with 18 U.S.C. §1734 solely to indicate this fact.

MATERIALS AND METHODS

Cloning of Human Mch4 and Mch5. Mch4 was cloned from human Jurkat λ Uni-ZAP XR cDNA library (Stratagene) (8). The primary PCR product obtained with the degenerate primers encoding the pentapeptide GSWFI/GSWYI and T3 vector-specific primer (9, 10) was used as a template for a secondary PCR amplification with primer T96-pr1 (TCAGCCTCGGCAGGAATAC) derived from GenBank accession no. T96912 and a second vector-specific primer SK-Zap (CAGGAATTCGGCACGAG) located downstream of the T3 primer. The products were cloned and then used as probes to screen the original Jurkat cDNA library. Positive λ clones were purified, rescued into the pBluescript II SK⁻ plasmid vector, and sequenced. While searching the GenBank database of human expressed sequence tags (ESTs) for sequences similar to Mch4, a 449-bp EST sequence (GenBank accession no. N42544) with a 64% identity to Mch4 was identified. Using PCR primers derived from the EST sequence (Mch5-pr1, GACAGAGCGAGATTCTGT; Mch5-pr2, GCACCATCAATCAGAAGG) and the vector-specific primers T3 and SK-zap, a cDNA (≈1.9 kb) corresponding to this gene was amplified with PCR from the Jurkat cDNA library and cloned in KS-vector. This cDNA was sequenced and its gene product was named Mch5.

Northern Blot Analysis. Tissue distribution analysis of Mch4 mRNA was performed on Northern blots (Clontech) using Mch4 cDNA as a probe as described previously (10).

Chromosomal Mapping of the *Mch4* Gene. A panel of DNAs from rodent–human somatic cell hybrids was screened by PCR with Mch4 specific primers t96-pr1 and t96-pr5 (CGGGAGATCATGTCTCAC). These primers were also used to screen by PCR the CEPH A and B yeast artificial chromosome libraries. A nonchimeric yeast artificial chromosome clone positive for Mch4 was used in fluorescence *in situ* hybridization analysis to probe normal human lymphocyte metaphases to sublocalize the *Mch4* gene.

Expression of Mch4 in Bacteria and Assay of Enzyme Activity. Mch4 cDNA lacking the two N-terminal FADD-like

Abbreviations: ASCP, aspartate-specific cysteine protease; Mch4 and Mch5, *m*ammalian *C*ed-3 *h*omolog nos. 4 and 5, respectively; ICE, interleukin 1β converting enzyme; CTL, cytotoxic T lymphocyte; EST, expressed sequence tag.

Data deposition: The sequences reported in this paper have been deposited in the GenBank data base (accession nos. U60519 and U60520).

§To whom reprint requests should be addressed at: Department of Pharmacology, Jefferson Medical College, Bluemle Life Sciences Building, 233 South 10th Street, Philadelphia, PA 19107. e-mail: E_Alnemri@lac.jci.tju.edu.

domains (amino acids 1–193) was subcloned in-frame into the *Bam*HI/*Xho*I sites of the bacterial expression vector pGEX-5X-3 (Pharmacia). Bacterial extracts were prepared and assayed as described (9, 10). The active GST-Mch4 enzyme (GST, glutathione *S*-tranferase) was purified from the bacterial extracts on glutathione–Sepharose and used for the gel cleavage assays as described below.

Purification of Granzyme B. Granzyme B was purified by immunopurification from human natural killer cell lysates using granzyme B-specific monoclonal antibody and assayed as described (20, 21).

Mutagenesis, *in Vitro* Transcription/Translation, and Cleavage Assays. Potential aspartate processing sites between the two subunits of ASCPs were mutated to alanine (CPP32 and Mch3) or glycine (Mch4) by site-directed mutagenesis using overlapping PCR mutagenic oligonucleotides. The resulting PCR products were subcloned in pBluescript II KS$^+$ vector under the T7 promoter and their sequences were verified by sequence analysis. Wild-type and mutated cDNAs were *in vitro* transcribed and translated in the presence of [^{35}S]methionine using Promega's coupled transcription/translation TNT kit according to the manufacturer's recommendations. Two microliters of the translation reactions were incubated with purified enzymes (100–200 ng) or with bacterial lysates expressing recombinant ASCPs in ICE-buffer, in a final volume of 10 μl. The reaction was incubated at 37°C for 1 hr and then analyzed by Tricine-SDS/PAGE and autoradiography.

RESULTS

Cloning of Mch4 and Mch5. A search of the GenBank data base ESTs for sequences related to CPP32 and Mch2 identified a short EST sequence (accession no. T96912). Based on this information, a 3.6-kb cDNA was cloned from human Jurkat T-lymphocyte cDNA library using a similar methodology as described (9, 10). This cDNA contains an open reading frame of 1437 bp that encodes a 479-amino acid protein, named Mch4, with a predicted molecular mass of ≈55 kDa (Fig. 1*A*). The size of the Mch4 mRNA (≈4 kb, see Fig. 2) and the presence of an in-frame stop codon 12 bp upstream from the initiator methionine indicates that the cloned Mch4 cDNA contains the full-length coding region. A search of the GenBank data base resulted in the identification of an EST (accession no. N42544) sequence with extensive homology to Mch4. This cDNA was cloned by PCR from the Jurkat cDNA library and sequenced. The new cDNA encodes a 496-amino acid protein, named Mch5, that is more related to Mch4 than to any other ASCP (Fig. 1).

Mch4 and Mch5 are Aspartate-Specific Cysteine Proteases of the Apoptotic CED-3 Subfamily. Previously identified ASCPs can be divided phylogentically into three subfamilies: (*i*) the Ced-3-like ASCP subfamily includes Ced-3, CPP32, Mch2, and Mch3 (8–10, 22); (*ii*) the ICE-like ASCP subfamily includes ICE, TX(ICH2, ICErel-II), and ICErelIII (8–10, 22); (*iii*) the NEDD-like subfamily includes ICH-1 and its mouse counterpart NEDD2 (6, 7). Mch4 and Mch5 belong to the Ced-3-like subfamily of ASCPs (Fig. 1*B*). Excluding the prodomain, Mch4 and Mch5 are equally related to Ced-3 (≈32% identity, 54% similarity). Mch4 is more related to Mch2 and Mch3 (≈38–40% identity, 56–58% similarity) than to CPP32 (≈35% identity, 57% similarity). On the other hand, Mch5 is equally related to CPP32, Mch2, and Mch3 (≈39–40% identity, 60–62% similarity). Mch4 and Mch5 are highly homologous to each other, with an overall ≈52% identity (67% similarity) at the primary amino acid sequence level, excluding the prodomain. The homology between the two proteins is highest within the small subunit region. A similar relationship was observed with other family members such as CPP32/Mch3 and ICE/TX. Like CPP32 and Mch3 (10), it is possible that Mch4 and Mch5 could heterodimerize with each other to form functional protease heterocomplexes. As with other known members of the family, expression of Mch4 in a heterologous system such as Sf9 insect cells resulted in apoptosis (data not shown).

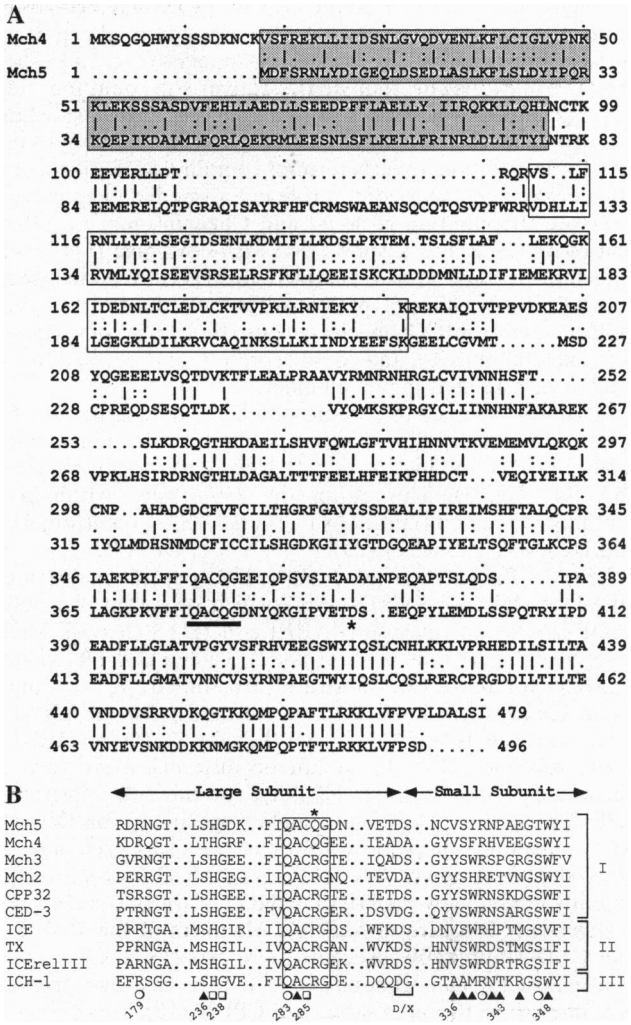

FIG. 1. Predicted amino acid sequences of proMch4 and proMch5 and their homology to other ASCP sequences. (*A*) Colinear alignment of proMch4 and proMch5 proteins. Dotted lines indicate gaps in the sequence to allow optimal alignment. Two FADD-like domains in proMch4 and proMch5 are boxed. The first domain (shaded) has the highest homology to the N-terminal 79 amino acid long FADD (GenBank accession no. U24231) death effector domain (37% identity, 57% similarity) than the second domain (22% identity, 53% similarity). First domain also shows high homology to PEA-15 (GenBank accession no. X86694) and KIAA0179 (GenBank accession no. D80001) proteins. Second domain shows some homology to SRB7 (GenBank accession no. U46837) and yeast cdc4 (GenBank accession no. Z46255) proteins. Active site QACQG is underlined. *, Asp-cleavage sites. Amino acid residues are numbered to the right of each sequence. (*B*) Multiple sequence alignment of all known human ASCPs and the nematode Ced-3 ASCP. The active site pentapeptide QACRG/QACQG is boxed. Based on crystal structure of ICE, the numbered residues within the ICE sequence are involved in catalysis (□), and binding the substrate-carboxylate of P1 Asp (○). ▲, The residues adjacent to the substrate P2-P4 amino acids. D/X indicates known and potential processing sites between the small and large subunits of ASCPs. The three ASCP-subfamilies are as follows: I, the Ced-like subfamily; II, the ICE-like subfamily, and III, the Nedd2/Ich-1 subfamily. *, The nonconservative Arg to Gln substitution in Mch4 and Mch5.

Like other ASCPs, mature Mch4 and Mch5 proteases are made of two subunits, derived from single polypeptide proenzymes (proMch4 and proMch5) by cleavage at highly conserved Asp residues (Asp372 in Mch4 and Asp391 in Mch5) located between the large and small subunits (Fig. 1*B*).

ProMch4 and proMch5 could also be processed further to remove the propeptide domains. Several potential aspartate cleavage sites are present in their prodomains (Fig. 1*A*). They are also unique in that their active site pentapeptide (QAC*Q*G) contains an Arg to Gln nonconservative substitution. This active site motif thus identifies a new subfamily of the ASCPs. In addition, their N termini contain FADD-like death effector domains, suggesting a role in Fas-mediated apoptosis.

Tissue Distribution of *Mch4* and Chromosomal Localization of its Gene. Fig. 2 shows that *Mch4* message (≈4 kb) is detectable in most tissues examined. Lowest expression is seen in whole brain, kidney, prostate, testis, and colon. Higher molecular mass mRNA species can also be seen in some tissues (i.e., skeletal muscle), and could represent unprocessed Mch4 mRNA or a related family member.

Mch4 was assigned to chromosome 2p12-qter using somatic cell hybrid analysis. Fluorescence *in situ* hybridization analysis further refined the localization of *Mch4* gene to chromosome 2q33–34 (Fig. 3). This places the *Mch4* gene within a 4 centimorgan region flanked by markers D2S374 (centromeric) and D2S346 (telomeric) (23).

Kinetic Parameters of Mch4. The peptide substrates DEVD-AMC and YVAD-AMC, which represent the poly-(ADP-ribose) polymerase (PARP) and IL-1β cleavage sites, respectively, were used in these assays (Table 1). The K_m values of Mch4 for these two substrates are similar. These values contrast with those for CPP32, where the K_m for the YVAD-AMC substrate is >35-fold higher than the K_m for the DEVD-AMC substrate (10). These kinetic differences are further illustrated by the ratio of V_{max}/K_m for the two substrates; CPP32 possesses a >500-fold higher specificity for DEVD-AMC substrate compared with Mch4 (ratios of 9200 and 18, respectively). However, like CPP32 and Mch3α (10), Mch4 is potently inhibited by the DEVD-CHO (24) (K_{iMch4} = 14 nM).

Granzyme B Activates Multiple Members of the Mammalian CED-3 Subfamily. Recently, granzyme B was shown to cleave proCPP32 to generate a ≈20 kDa cleavage product presumed to be the large subunit of CPP32 (16). This cleavage was suggested to occur at the processing sequence IETD-S between the two subunits of CPP32, but no direct evidence was presented. The potential processing sequences between the two subunits of Mch3 and Mch4 are similar to that of CPP32 (Fig. 1*B*). These sequences contain identical P1 (CPP32-D175, Mch3-D198, and Mch4-D372) and P4 (CPP32-I172, Mch3-I195, and Mch4-I369) residues in all three proenzymes and a conserved P3 residue (CPP32-E173, Mch3-Q197, and Mch4-E370). To determine whether granzyme B can cleave these proenzymes at the proposed processing sites, mutant proenzymes with a P1 D to A substitution (in CPP32 and Mch3) or a D to G (in Mch4) were generated. Parental and mutant proenzymes were *in vitro* translated in the presence of [^{35}S]methionine, incubated with purified granzyme B and then analyzed by SDS/PAGE and autoradiography. As shown in Fig. 4*A*, *in vitro* translation of wild-type (lane 1) or Asp175-mutated (lanes 2 and 3) CPP32 proenzymes generated identical pattern of translation products. The major translation product corresponding to full-length proCPP32 migrates as a 32–33 kDa band. The two minor ≈29 and ≈27 kDa bands are most likely internal translation products starting with Met27 and Met39, respectively. Incubation of these translation products with granzyme B resulted in cleavage of the wild-type proCPP32 at Asp175 (lane 5) to generate the two subunits of active CPP32. The small C-terminal subunit migrates as a single ≈12-kDa band and the large N-terminal subunit migrates as three bands (≈20, ≈19, and ≈17 kDa). The faint ≈20 kDa band is most likely a cleavage product of the full-length proCPP32. How-

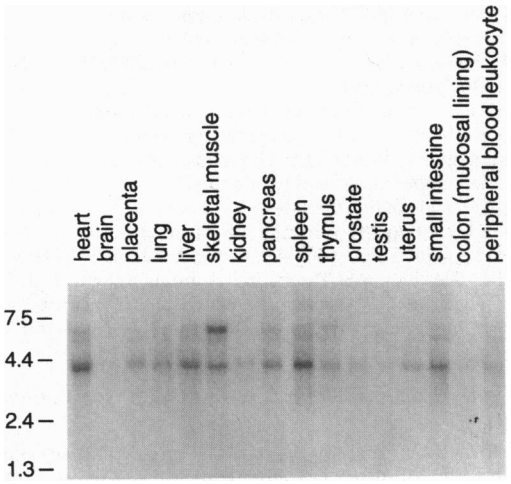

FIG. 2. Tissue distribution of human Mch4 mRNA. Northern blot analysis of human tissue poly(A)$^+$ RNA (2 μg per lane) using the full-length Mch4 as a probe. Molecular mass markers in Kb are shown on the left.

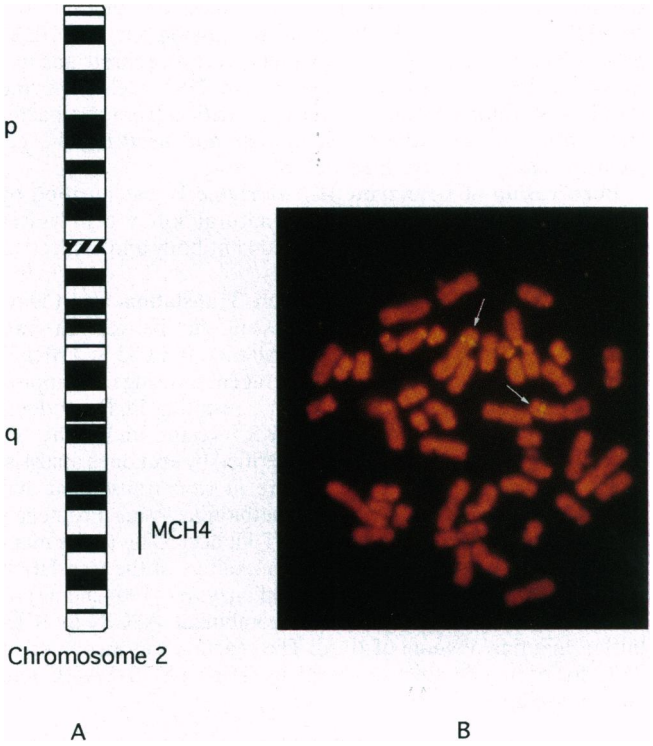

FIG. 3. Chromosomal localization of Mch4 gene. (*A*) Idiogram of chromosome 2 showing the position of the Mch4 gene marked by a vertical line to the right of the idiogram. (*B*) Propidium iodide image of fluorescence *in situ* hybridization analysis on normal lymphocyte metaphases with Mch4 positive yeast artificial chromosome clone 828E8. Arrows mark chromosome 2 where hybridization signals are visible at 2q33-34.

Table 1. Kinetic parameters of Mch4

Parameter	Value
K_m (DEVD-AMC)	130 μM
K_m (YVAD-AMC)	150 μM
K_i (DEVD-CHO)	14 nM
V_{max}/K_m (DEVD-AMC)	18

The activity of recombinant Mch4 was measured using bacterial lysates prepared with ICE buffer (25 mM Hepes/1 mM EDTA/5 mM dithiothreitol/0.1% CHAPS/10% sucrose, pH 7.5) at room temperature. The K_i values were determined from the hydrolysis rate of 50 μM DEVD-AMC after a 30-min preincubation of the enzyme with inhibitor (DEVD-CHO).

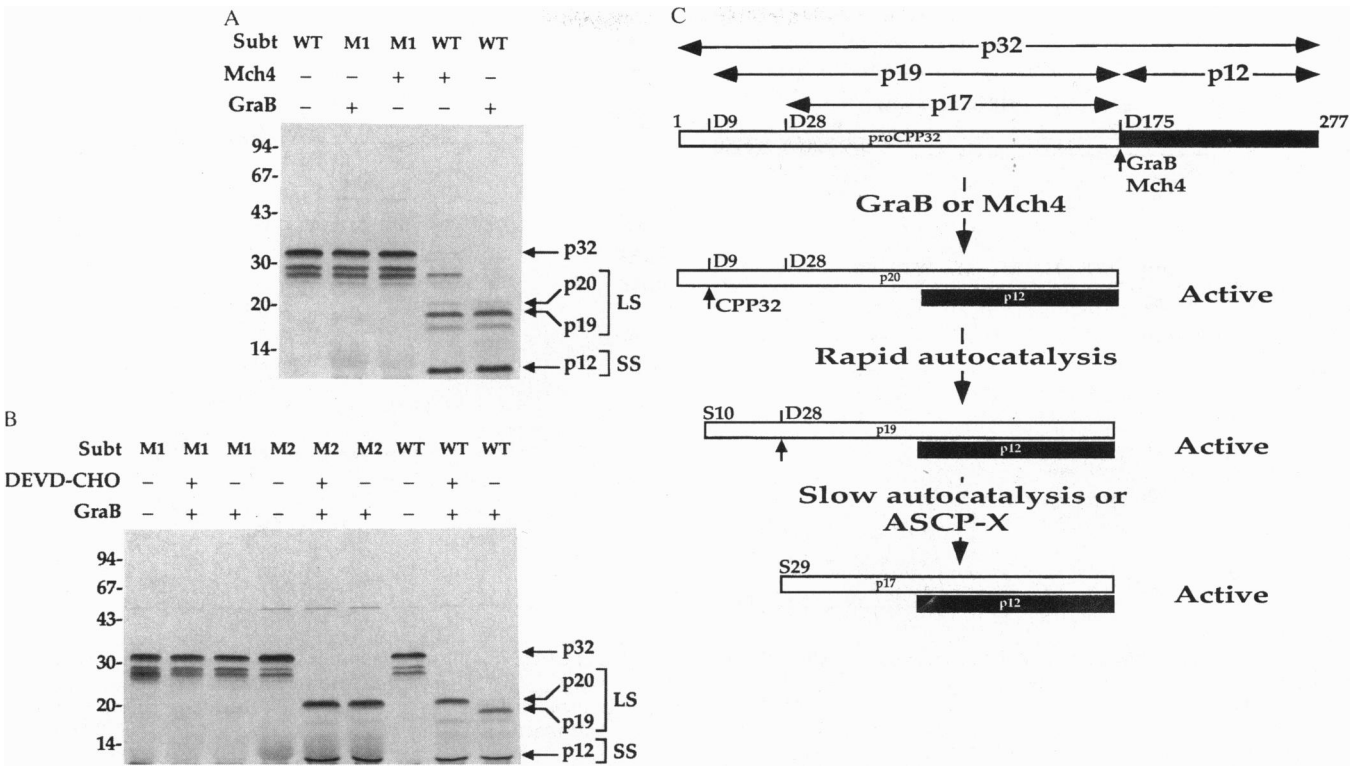

FIG. 4. Cleavage of CPP32 proenzyme by Mch4 and granzyme B. Effect of Asp175 mutation (*A*) or Asp9 mutation and the DEVD-CHO inhibitor (*B*) on cleavage of of proCPP32. ^{35}S-labeled wild-type proCPP32 (WT lanes), Asp175-mutated proCPP32 (M1 lanes), or Asp9-mutated (M2 lanes) were incubated with purified recombinant Mch4 (Mch4, + lanes), purified granzyme B (GraB, + lanes), or buffer (Mch4 and GraB, – lanes) in the presence (+ lanes) or absence (– lanes) of the DEVD-CHO (0.4 μM) inhibitor for 1 hr at 37°C. The reaction products were then analyzed by SDS/PAGE and autoradiography. (*C*) Diagram illustrating the three-step mechanism of activation/processing of CPP32 by granzyme B and Mch4. Subt, substrate; SS, the small subunit; LS, the large subunit.

ever, the high intensity of the ≈19-kDa band suggests that it is produced from the ≈20-kDa band by further processing of the prodomain. This is supported by the observation that cleavage of proCPP32 by granzyme B in the presence of a potent CPP32 peptide inhibitor, DEVD-CHO, generated the ≈20-kDa band, which was not further processed to the ≈19-kDa band (Fig. 4*B*, lane 8). Further processing of the ≈20-kDa band to the ~19-kDa band was only observed in the absence of the peptide inhibitor DEVD-CHO (Fig. 4*A*, lane 5 and Fig. 4*B*, lane 9). Thus, additional processing of the prodomain is most likely due to the autocatalytic activity of the granzyme B-activated CPP32. No cleavage was observed with the buffer control or the Asp175-mutated CPP32 (Fig. 4*A*, lanes 1 and 2, respectively). There was also no cleavage at the prodomain of the Asp175-mutated CPP32 (Fig. 4*A*, lane 2 and Fig. 4*B*, lane 3), supporting our earlier conclusion that cleavage of the prodomain is an autocatalytic activity of activated CPP32. The ≈17-kDa band is a cleavage product of one of the smaller internally translated products, most likely the 29-kDa band.

The observed autocatalytic processing within the prodomain of CPP32 occurs at Asp9 and not at Asp28. Mutation of Asp9 to Ala inhibited the processing of the ≈20-kDa band to the ≈19-kDa band as observed with the DEVD-CHO inhibitor (Fig. 4*B*, lanes 5 and 6). Thus, active CPP32 processes itself at Asp9 after activation to generate a p19 (large subunit) and p12 (small subunit) (Fig. 4*C*). This autocatalytic activity is rapid and occurs immediately after proCPP32 is cleaved at Asp175. Previously reported cleavage at Asp28 (24) could be due to a slow autocatalytic activity of active CPP32 or an activity of another ASCP. We observed that purified recombinant CPP32 expressed in bacteria undergoes slow autoprocessing to the 17-kDa subunit after prolonged incubation at 37°C (data not shown).

Similarly, *in vitro* translation of wild-type (Fig. 5*A*, lane 1) or Asp198-mutated proMch3 (Fig. 5*A*, lane 2) generated two major products; a 35- to 36-kDa product corresponding to the full-length proMch3 and a 30-kDa internal translation product most likely starting with Met45. Other translation products smaller than 30 kDa can also be seen. Like proCPP32, incubation of proMch3 with granzyme B generated the two subunits of the active Mch3 enzyme (Fig. 5*A*, lane 6). These subunits can be seen as a ≈12-kDa band corresponding to the small C-terminal subunit and two ≈20- and ≈18-kDa bands corresponding to the large N-terminal subunit. The ≈20-kDa band is a product of processing at Asp198 between the two subunits and at Asp23 in the propeptide domain (10). The ≈18-kDa band is most likely a cleavage product of the smaller 30-kDa internally translated product. No cleavage products corresponding to the small or large subunits were observed with the buffer control or the Asp198-mutated proMch3 (Fig. 5*A*, lanes 1, 2, and 4, respectively). Unlike CPP32, there was a 33-kDa cleavage product in the Asp198-mutated proMch3 (lane 4), possibly resulting from granzyme B cleavage at Asp23 in the propeptide domain of proMch3. Thus, granzyme B processing of Mch3 could differ from that of CPP32 by processing proMch3 to active Mch3 both between the large and small subunits and within the propeptide domain. We have shown recently that CPP32 can also cleave the propeptide domain of proMch3 efficiently (10). Thus, activation of CPP32 *in vivo* by granzyme B could result in further processing of both CPP32 and its closely related homolog Mch3.

Two truncated proMch4 lacking the N-terminal FADD-like domains were used to analyze cleavage of proMch4 by granzyme B. ProMch4-M134 starts with M134 and ProMch4-M235 starts with M235. *In vitro* translation of ProMch4-M134 (Fig. 5*B*, lane 4) or Asp372-mutated proMch4-M134 (Fig. 5*B*, lane 5) generated two major products: a 39-kDa product and a 27-kDa internal translation product. The internally translated product starts with Met235 and it is identical to truncated ProMch4-M235 (Fig. 5*B*).

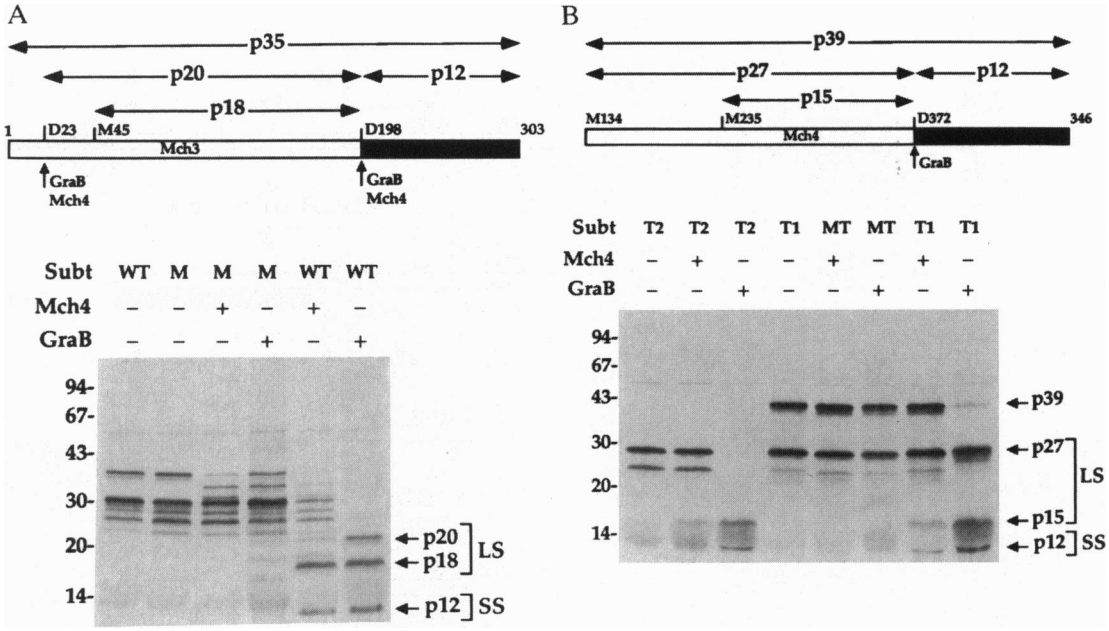

FIG. 5. Cleavage of Mch3 and Mch4 proenzymes by Mch4 and granzyme B. (*A*) Effect of aspartate mutations on cleavage of proMch3 (*A*) or proMch4 (*B*). ^{35}S-labeled wild-type proMch3 (WT lanes), Asp198-mutated proMch3 (M lanes), truncated proMch4-M134 (T1 lanes), truncated proMch4-M235 (T2 lanes), or Asp372-mutated proMch4-M134 (MT lanes) were incubated with recombinant Mch4 (Mch4, + lanes), granzyme B (GraB, + lanes), or buffer (Mch4 and GraB, − lanes) for 1 hr at 37°C. The reaction products were then analyzed by SDS/PAGE and autoradiography. SS, the small subunit; LS, the large subunit.

Granzyme B cleaved ProMch4-M235 to generate 15- to 16-kDa and 12-kDa bands (lane 3). It also cleaved ProMch4-M134 to generate ≈27-kDa band and 12-kDa band (lane 8). The 12-kDa band is the C-terminal small subunit of Mch4. However, because of the presence of the internally translated 27-kDa protein together with proMch4-M134, a 15- to 16-kDa band is also produced after incubation with granzyme B (lane 8). Like CPP32 and Mch3, the Asp372-mutated proMch4-M134 was not cleaved by granzyme B (lane 6), and there was no cleavage in the buffer controls (lanes 1 and 4).

These data provide the first direct evidence that granzyme B activates pro-CPP32, Mch3, and Mch4 by cleavage at the IETD-S, IQAD-A, and IEAD-A sequences, respectively.

Mch4 Processes CPP32 and Mch3 Proenzymes *in Vitro*. Evidence suggests that CPP32 might be a downstream protease activated by proteases such as ICE and granzyme B. ICE itself does not appear to be critical for apoptosis execution in several model systems, and cells undergo apoptosis in most instances independently of granzyme B. Both proMch4 and proMch5 contain N-terminal FADD-like death effector domains. The N-terminal death effector domain of FADD (19) may bind one of the two FADD-like domains in proMch4 or proMch5 for activation and recruitment to Fas-apoptotic pathway. Activation of proMch4 or proMch5 by FADD may lead to activation of downstream proteases such as CPP32 and Mch3. To test whether CPP32 and its closely related homolog Mch3 can be activated by Mch4, purified recombinant Mch4 was incubated with proCPP32 and proMch3. Mch4 processed proCPP32 and proMch3 and generated cleavage products identical to those produced by granzyme B (Fig. 4*A*, lane 4 and Fig. 5*A*, lane 5). Mch4 was unable to process the Asp to Ala mutated proCPP32 or proMch3 (Fig. 4*A*, lane 3 and Fig. 5*A*, lane 3), demonstrating that Mch4 and granzyme B use the same sites for cleavage of CPP32 and Mch3. However, like granzyme B, Mch4 was able to cleave the propeptide of Mch3 to generate a 33-kDa band (Fig. 5*A*, lane 3), which was further processed in the wild-type Mch3 to the ≈20- and 12-kDa bands, although to a lesser extent than with granzyme B (lanes 5 and 6). A longer incubation (>1 hr) resulted in complete conversion of the 33-kDa band to the 20-kDa band (data not shown). Although Mch4 was able to cleave proMch4-M134, its activity toward its proenzyme was significantly lower than that toward proCPP32 and proMch3 (Fig. 5*B*, lane 7). In addition, there was no significant cleavage of proMch4-M134 when incubated with recombinant CPP32 or Mch3 enzymes (data not shown). ASCPs such as ICE, TX, and Mch2 were also unable to efficiently process proMch4-M134 (data not shown). Consequently, Mch4 may be upstream of CPP32 and Mch3 in the mammalian apoptotic protease cascade.

DISCUSSION

ASCPs have two unique features that distinguish them from other proteases. They all cleave their substrates after Asp residues and their activation requires cleavage after Asp residues located in highly conserved processing sites between their large and small subunits and in their prodomain. The small subunit is derived from the C terminus of the proenzyme. The mature large subunit is then generated by processing of the remaining N-terminal prodomain. The ability to cleave after Asp residues is only shared with granzyme B, a serine protease that does not, however, require cleavage after Asp residues for its activation. These features suggest that ASCPs could interact with and activate each other in a protease cascade fashion and could also be substrates for granzyme B. In addition, because multiple ASCP family members coexist in one cell type (i.e., Jurkat T-lymphocytes), the ability of one family member to activate several other family members and vice versa could generate an amplifiable protease cascade(s). Different ASCP cascades may operate in different cell types, because some members of the ASCP family are expressed in a tissue-specific manner, and there is redundancy within this family.

We can envision at least three ASCP activation pathways (Fig. 6). One of these pathways involves Mch4 acting upstream of CPP32, Mch2, and Mch3. Once Mch4 is activated by certain apoptotic stimuli, it can process and activate the proenzymes of Mch3 and CPP32, the two ASCPs possibly responsible for poly-(ADP-ribose) polymerase cleavage in apoptosis (8–10, 24, 25). Active CPP32 can in turn activate proMch2, the only ASCP that can cleave lamin (unpublished observations and ref. 26). Presumably, such a pathway would not be affected in ICE-knockout mice.

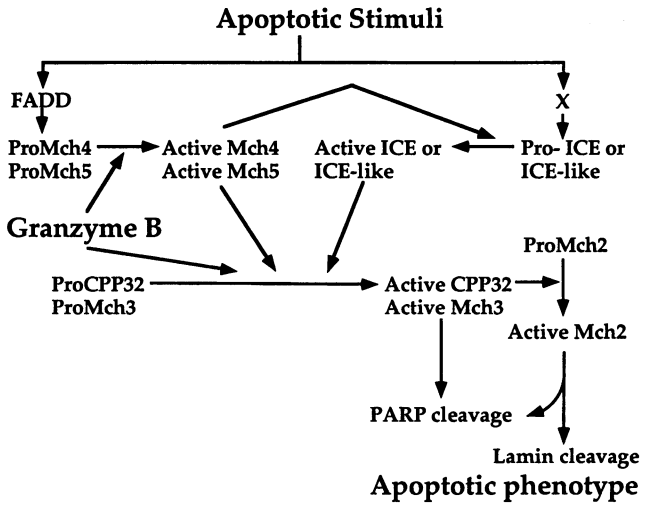

FIG. 6. Potential apoptotic protease pathways involving activation of multiple ASCP family members. See text for details.

In an alternative ICE or an ICE-like pathway, activation of ICE or an ICE-like ASCP like TX by an apoptotic stimulus or an upstream ASCP would result in CPP32, Mch2, and Mch3 activation. This is because TX can activate ICE (11) and ICE can activate proCPP32 (25). This ICE-like pathway might be operating in the Fas-apoptotic pathway, because ICE knockout or CrmA abrogate this pathway in some cell types (27–29). Also, during Fas-induced apoptosis, an ICE-like activity precedes CPP32-like activity (30). Consequently, FADD may bind the FADD-like domain in proMch4 or proMch5 for activation and recruitment to Fas-apoptotic pathway. This is because these domains are capable of both homotypic and heterotypic interactions (17–19). Once bound to FADD, the proenzymes may undergo autocatalytic processing to the mature enzymes. Mature Mch4 or Mch5 could activate proCPP32 directly, or indirectly by activating proTX. We observed that Mch5 can process proCPP32 and proTX (data not shown). Mature CPP32 can in turn activate the lamin-cleaving enzyme Mch2.

The most N-terminal or first domain in proMch4 and proMch5 (Fig. 1) is highly related to FADD and may act as activator of the proenzymes by binding the second C-terminal FADD-like (interacting) domain. We speculate that these proteases may mediate Fas apoptosis by interacting with FADD. However, because they have their own N-terminal FADD domain, they may be involved in other forms of apoptosis. ProMch4 and proMch5 might be repressed under normal conditions by a repressor that sits on their N-terminal FADD domain. Alterations in cellular conditions could release the repressor, allowing the N-terminal domain to interact with the second C-terminal FADD-interacting domain, leading to their activation and, consequently, activation of downstream proteases such as CPP32, Mch3, and Mch2.

The granzyme B pathway is another distinct apoptotic protease pathway used by CTLs to kill their target cells. We demonstrate that granzyme B not only activates proCPP32, but it can also activate proMch3 and proMch4 (Figs. 4 and 5) and the newly identified proMch5 (data not shown). This is not surprising because the potential cleavage site in proMch5 is highly related to that of proCPP32 (VETD-S versus IETD-S, respectively). There is evidence that CTLs use both Fas-ligand/Fas interaction and the granzyme B pathways to insure killing of their target cells (31, 32). These multiple pathways must have evolved in higher eukaryotes to insure elimination of cells during normal developmental or in pathological conditions. Although it now appears that ASCPs are components of an amplifiable protease cascade, it is of great interest to determine how proMch4 and proMch5 are activated in pathways that are independent of granzyme B. Furthermore, it is important to determine whether FADD can interact directly with proMch4 and proMch5, and whether this interaction could lead to their activation.

This work was supported in part by a research grant from IDUN Pharmaceuticals to E.S.A. and by the National Institutes of Health Research Grant AI 35035 to G.L.

1. Ellis, R. E., Yuan, J. & Horvitz, H. R. (1991) *Annu. Rev. Cell Biol.* **7,** 663–698.
2. Raff, M. C. (1992) *Nature (London)* **356,** 397–400.
3. Wyllie, A. H. (1980) *Int. Rev. Cytol.* **68,** 251–307.
4. Thornberry, N. A., Bull, H. G., Calaycay, J. R., Chapman, K. T., Howard, A. D., *et al.* (1992) *Nature (London)* **356,** 768–774.
5. Cerretti, D. P., Kozlosky, C. J., Mosley, B., Nelson, N., Van Ness, K., Greenstreet, T. A., March, C. J., Kronheim, S. R., Druck, T., Cannizzaro, L. A., Huebner, K. & Black, R. A. (1992) *Science* **256,** 97–100.
6. Kumar, S., Kinoshita, M., Noda, M., Copeland, N. G. & Jenkins, N. A. (1994) *Genes Dev.* **8,** 1613–1626.
7. Wang, L., Miura, M., Bergeron, L., Zhu, H. & Yuan, J. (1994) *Cell* **78,** 739–750.
8. Fernandes-Alnemri, T., Litwack, G. & Alnemri, E. S. (1994) *J. Biol. Chem.* **269,** 30761–30764.
9. Fernandes-Alnemri, T., Litwack, G. & Alnemri, E. S. (1995) *Cancer Res.* **55,** 2737–2742.
10. Fernandes-Alnemri, T., Takahashi, A., Armstrong, R., Krebs, J., Fritz, L., Tomaselli, K. J., Wang, L., Yu, Z., Croce, C. M., Earnshaw, W. C., Litwack, G. & Alnemri, E. S. (1995) *Cancer Res.* **55,** 6045–6052.
11. Faucheu, C., Diu, A., Chan, A. W., Blanchet, A. M., Miossec, C., Herve, F., Collard-Dutilleul, V., Gu, Y., Aldape, R. A., Lippke, J. A., Rocher, C., Su, M. S.-S., Livingston, D. J., Hercend, T. & Lalanne, J.-L. (1995) *EMBO J.* **14,** 1914–1922.
12. Kamens, J., Paskind, M., Hugunin, M., Talanian, R. V., Allen, H., Banach, D., Bump, N., Hackett, M., Johnston, C. G., Li, P., Mankovich, J. A., Terranova, M. & Ghayur, T. (1995) *J. Biol. Chem.* **270,** 15250–15256.
13. Munday, N. A., Vaillancourt, J. P., Ali, A., Casano, F. J., Miller, D. K., Molineaux, S. M., Yamin, T. T., Yu, V. L. & Nicholson, D. W. (1995) *J. Biol. Chem.* **270,** 15870–15876.
14. Henkart, P. A. (1996) *Immunity* **4,** 195–201.
15. Steller, H. (1995) *Science* **267,** 1445–1448.
16. Darmon, A. J., Nicholson, D. W. & Bleackley, R. C. (1995) *Nature (London)* **377,** 446–448.
17. Boldin, M. P., Varfolomeev, E. E., Pancer, Z., Matt, I. L., Camonis, J. H. & Wallach, D. (1995) *J. Biol. Chem.* **270,** 7795–7798.
18. Chinnaiyan, A. M., O'Rourke, K., Tewari, M. & Dixit, V. M. (1995) *Cell* **81,** 505–512.
19. Hsu, H., Shu, H.-B., Pan, M.-G. & Goeddel, D. V. (1996) *Cell* **84,** 299–308.
20. Trapani, J. A., Browne, K. A., Dawson, M. & Smyth, M. J. (1993) *Biochem. Biophys. Res. Commun.* **195,** 910–920.
21. Trapani, J. A., Smyth, M. J., Apostolidis, V. A., Dawson, M. & Browne, K. A. (1994) *J. Biol. Chem.* **269,** 18359–18365.
22. Yuan, J., Shaham, S., Ledoux, S., Ellis, H. M. & Horvitz, H. R. (1993) *Cell* **75,** 641–652.
23. Chumakov, I., Rigault, P., Le Gall, I., Bellanne-Chantelot, Billault, A., *et al.* (1995) *Nature (London)* **377.** Suppl., 175–183.
24. Nicholson, D. W., Ali, A., Thornberry, N. A., Vaillancourt, J. P., Ding, C. K., Gallant, M., Gareau, Y., Griffin, P. R., Labelle, M., Lazebnik, Y. A., Munday, N. A., Raju, S. M., Smulson, M. E., Yamin, T.-T., Yu, V. L. & Miller, D. K. (1995) *Nature (London)* **376,** 37–43.
25. Tewari, M., Quan, L. T., O'Rourke, K., Desnoyers, S., Zeng, Z., Beidler, D. R., Poirier, G. G., Salvesen, G. S. & Dixit, V. M. (1995) *Cell* **81,** 801–809.
26. Takahashi, A., Alnemri, E. S., Lazebnik, Y. A., Fernandes-Alnemri, T., Litwack, G., Moir, R. D., Goldman, R. D., Poirier, G. G., Kaufmann, S. H. & Earnshaw, W. C. (1996) *Proc. Natl. Acad. Sci. USA,* in press.
27. Kuida, K., Lippke, J. A., Ku, G., Harding, M. W., Livingston, D. J., Su, M. S.-S. & Flavell, R. A. (1995) *Science* **267,** 2000–2003.
28. Enari, M., Hug, H. & Nagata, S. (1995) *Nature (London)* **375,** 78–81.
29. Los, M., Van de Craen, M., Penning, L. C., Westendorp, M., Baeuerle, P. A., Droge, W., Krammer, P. H., Fiers, W. & Schulze-Osthoff, K. (1995) *Nature (London)* **375,** 81–83.
30. Enari, M., Talanian, R. V., Wong, W. W. & Nagata, S. (1996) *Nature (London)* **380,** 723–726.
31. Kaegi, D., Vignaux, F., Ledermann, B., Buerki, K., Depraetere, V., Nagata, S., Hengartner, H. & Golstein, P. (1994) *Science* **265,** 828–530.
32. Lowin, B., Hahne, M., Mattmann, C. & Tschopp, J. (1994) *Nature (London)* **370,** 650–652.